JOURNAL OF MATERIALS SCIENCE **34** (1999) 1497–1503

Non-destructive studies on tensile and fracture properties of molybdenum at low temperatures (148 to 423 K)

M. D. MATHEW, K. L. MURTY
North Carolina State University, Raleigh, NC 27695-7909, USA
E-mail: mdmathew@eos.ncsu.edu

Tensile and fracture properties of molybdenum have been studied using the automated ball indentation technique. Tests have been carried out at several temperatures in the range of 148 to 423 K at a constant strain rate. Tensile properties determined from these tests agreed well with published results from conventional tensile tests. Temperature dependence of indentation energy to fracture, the fracture toughness parameter specific to this technique using critical stress-to-fracture concept, showed a sharp transition from brittle to ductile condition. These results complement the previous studies on pressure vessel steels, and clearly demonstrate that automated ball indentation technique is a reliable and non-destructive method for determining tensile and fracture properties of materials.

1. Introduction

Stress-Strain Microprobe (SSM) is a newly developed equipment that can be used for determining the mechanical properties and fracture behavior of materials in a nearly non-destructive manner [1]. SSM employs the principle of Automated Ball Indentation (ABI) technique. Studies using SSM clearly demonstrated the feasibility of obtaining the true stress-strain behaviors of ferritic steels and weldments (and of different microstructural regions such as heat-affected zones), stainless steel castings as well as electronic solders (SnSb, AgSn etc.) [2–6]. The fracture properties have been evaluated in terms of a new fracture energy parameter called Indentation Energy to Fracture (IEF) using critical stress-to-fracture concept [7]. Good correlation has been obtained between ABI, tensile and impact tests on various materials under different thermo-mechanical conditions [2–7].

In this paper, we report the tensile and fracture properties of commercially pure molybdenum metal over a temperature range of 148 to 423 K as determined from ABI tests. A small rod of 12.5 mm diameter was used for these tests. The principles of ABI technique are briefly described in the following section.

2. Stress-strain microprobe

Although the principle of ball indentation to study deformation behavior of materials is not new [8, 9], ABI technology has several distinctly unique features. The foremost feature is that it is fully automated and does not require measurement of diameter of the indentation after testing using elaborate profilometry, optical interferometry etc. that renders the traditional methodology unsuitable for on-line measurement of the mechanical properties of structures in-service. The Stress-Strain Microprobe System was developed and patented by Advanced Technology Corporation [1] to test minimal material, and determine several mechanical property parameters of metallic structures including welds and heat-affected zones. The SSM system is based on the principle of strain-controlled multiple indentations at a single penetration location on a polished surface by a small spherical indenter (diameter equal to or less than about 1.57 mm). The indentation depth is progressively increased to a maximum user-specified limit with intermediate partial unloadings. The applied indentation loads and associated penetration depths are measured during the test and are used to calculate the incremental stress-strain values from a combination of elasticity and plasticity theories, and semi-empirical relationships which govern material behavior under multiaxial indentation loading [3, 6]. By analyzing the flow curve, tensile parameters of the material such as yield strength, ultimate tensile strength, strength coefficient and strain hardening exponent, as well as a fracture energy parameter called Indentation Energy to Fracture (IEF) are evaluated.

One of the greatest advantages of ABI technique is that it is nearly non-destructive since no material is removed from the testing surface. A smooth shallow spherical indentation, as small as 0.5 mm deep is left at the end of the test. This spherical impression is harmless to the tested structure because it has no sharp edges, and so it does not introduce any stress concentration sites. Moreover, the ball indentation leaves a compressive residual stress which will retard crack initiation at the ABI test site. Because of the small area over

which the test is carried out, it is possible to determine point to point variations in mechanical properties (such as those that exist between base metal, heat affected zone and weld nugget in a weldment). Although ABI technique is non-intrusive/non-destuctive, it is a state-of-the-art mechanical test that measures directly the current/local deformation (stress-strain) behavior of the material. Hence, SSM can be used as an *in-situ* testing instrument for non-destructive assessment of mechanical properties of components in-service (e.g. nuclear, chemical, aerospace, and defense) without adversely affecting their structural integrity.

The SSM system uses an electro-mechanically driven indenter, high resolution penetration transducer and load cell, a personal computer (PC), a 16-bit data acquisition/control unit, and a copyrighted ABI software. The test is fully automated with a PC and test controller used in innovative ways to control the test and analyze data including real-time graphics, digital display of load-depth test data, etc. Fig. 1 shows an overall view of the SSM system. Spherical indenters made of tungsten carbide are used with diameters varying from 0.254 to 1.575 mm, depending on the specimen thickness and width of the microstructural region to be tested. The indenter is driven at a constant speed into the material to be tested, and progressive multiple loadings/partial unloadings are performed at a single test location. Load and depth of penetration are monitored using on-line load cell and linear variable differential transducer respectively. Capability of the system has been further improved recently by incorporating single cycle test method with no intermediate partial unloadings; such tests are required for high strain rate testing and continuous stress-strain measurement. Low and high temperature testing capability has been added with a furnace and temperature controller that enables testing in the range of 73 to 473 K.

3. ABI analysis

3.1. Yield strength

In a standard tensile test, the uniaxial deformation is confined to the constant volume of the specimen's gauge section. Initially, the material is deformed elastically, following which plastic yielding and work-hardening commence and continue uniformly till the

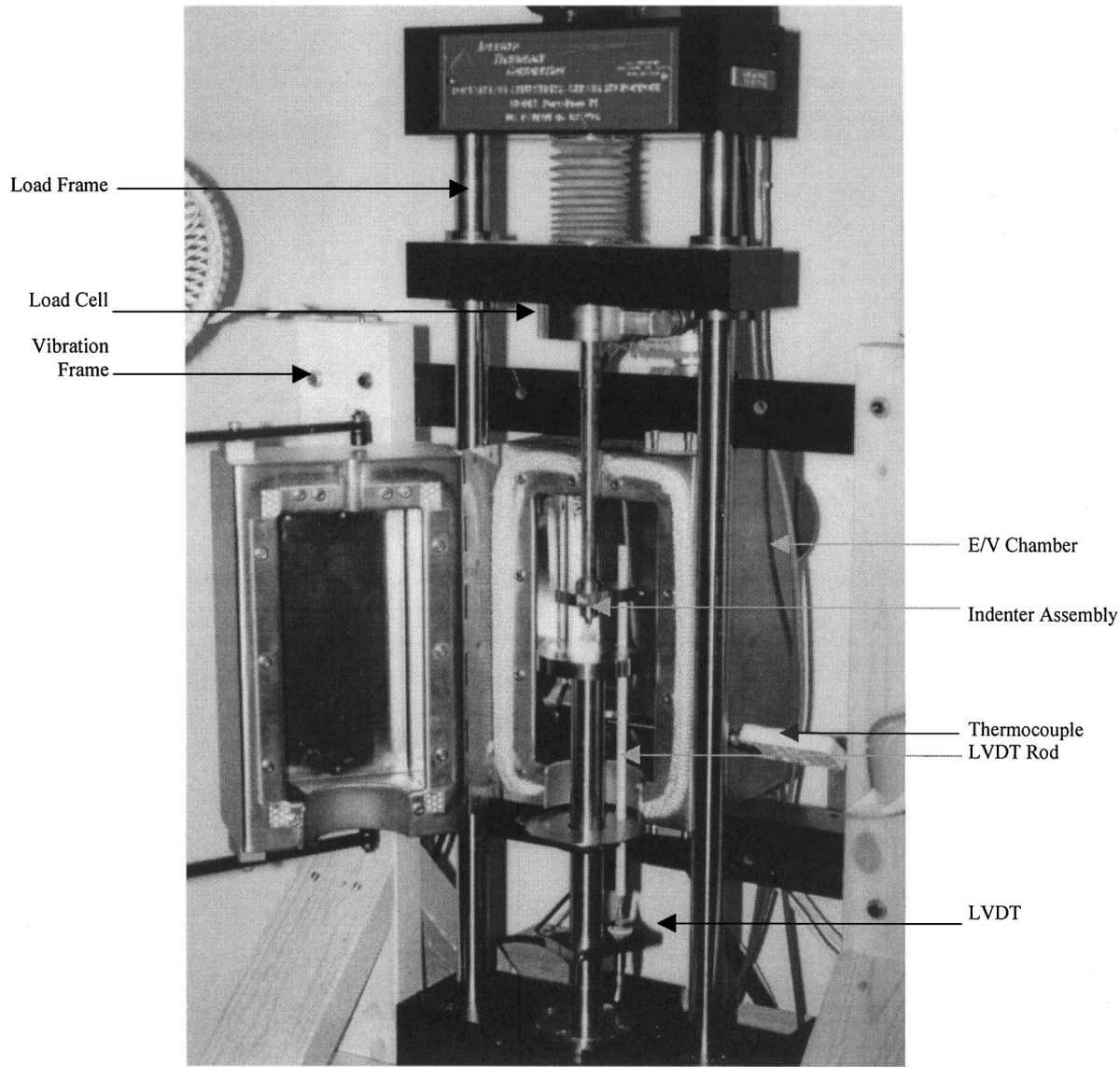

Figure 1 Stress-Strain Microprobe System with environmental chamber.

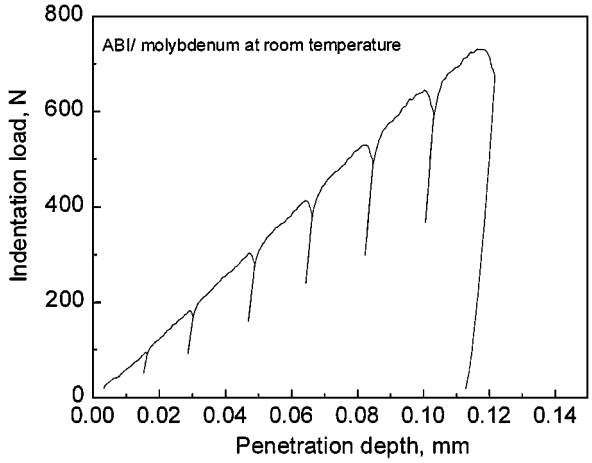

Figure 2 Typical indentation load versus depth curve at room temperature.

onset of necking. In contrast, in an ABI test, the elastic and plastic deformations are not distinctly separated. With increasing indentation penetration depth, an increasing volume of test material is forced to flow under multiaxial compressive stresses generated by the advancing indenter. Hence, in an ABI test, yielding and work-hardening occur simultaneously during the whole course of the test. An accurate determination of yield strength should hence be based on the entire load-displacement curve from the ABI test. It should be emphasized that in an ABI test consisting of seven loading and unloading cycles as shown in Fig. 2, there will be seven consecutive processes of work hardening of both old and new material. Hence, the yield strength analysis is carried out by taking into account simultaneous occurrence of yielding and strain hardening of the material under conditions of multiaxial compression.

As seen from Fig. 2, ABI load increases linearly with penetration depth. The linear increase is the consequence of two non-linear but opposing processes occurring simultaneously, i.e. the non-linear increase of load with depth due to spherical geometry of the ball indenter and increase of load due to power-law work hardening of the material. Hence, ABI tests do not exhibit the traditional segmented behavior, i.e., linear elastic followed by non-linear work-hardening of the material. Fig. 3 shows a schematic representation of the indentation profile in an ABI test. For each ABI loading cycle, the total penetration depth (h_t) is measured while the load is applied and the depth is converted to a total indentation diameter (d_t) using the following equation:

$$d_t = 2\sqrt{Dh_t - h_t^2} \tag{1}$$

In Equation 1, D is the diameter of the indenter. The plastic depth, h_p, is derived by extrapolating total depth to zero load. Data points from all loading cycles (maximum value of $d_t/D = 1.0$) are fit by linear regression analysis to the following relationship:

$$P/d_t^2 = A(d_t/D)^{m-2}, \tag{2}$$

where P is the applied indentation load, m is the Meyer's coefficient and A is a material parameter obtained from the regression analysis. Knowing the material parameter A, the yield strength (σ_y) is calculated from the expression:

$$\sigma_y = \beta_m A \tag{3}$$

where β_m is a constant for a given class of materials. The value of β_m for each class of materials is determined independently using yield strength obtained from standard tensile tests, and value of A obtained from ABI tests. A single value of 0.2285 for β_m has been found to be applicable to all carbon steels whether cold rolled, hot rolled or irradiated [2–5].

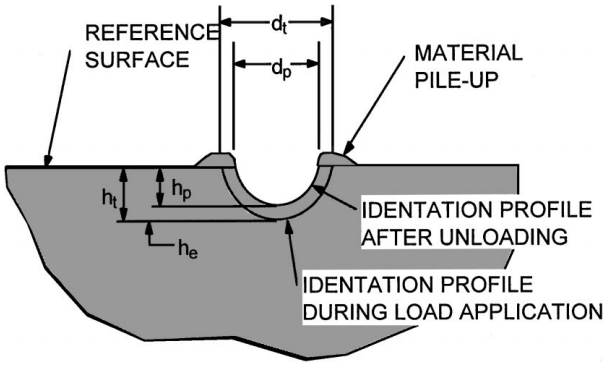

Figure 3 ABI indentation geometry.

3.2. Stress-strain relation

A basic premise in the application of the ABI technique is that materials behave similarly under tensile and compressive loading. Plastic flow of materials under tensile loading is generally represented by the equation

$$\sigma_t = K\varepsilon_p^n, \tag{4}$$

where σ_t is the true stress, ε_p is the true plastic strain, n is the strain hardening exponent and K is the strength coefficient. This representation is not a necessary requirement for determining the indentation-derived $\sigma_t - \varepsilon_p$ curve as will be shown later (Equations 6 and 7) but it can be used to determine n over the ε_p range of interest. Besides, a single power law curve may not fit the entire flow curve as noted in ASTM Standard E646-78 (Standard Test Method for Tensile Strain Hardening Exponents of Metallic Sheet Materials).

A computer program is used to solve the following equations to determine the true stress and true strain values. From the plastic depth h_p, the plastic diameter d_p is calculated by iterating the following equation,

$$d_p = \sqrt[3]{(2.735PD)\frac{(1/E_{spec} + 1/E_{ind})(4h_p^2 + d_p^2)}{4h_p^2 + d_p^2 - 4h_pD}} \tag{5}$$

where P is the measured load, E_{spec} and E_{ind} are the elastic moduli of the specimen and indenter

respectively. The true stress (σ_t) and plastic strain (ε_p) values are then calculated using the following equations,

$$\varepsilon_p \equiv 0.2\frac{d_p}{D} \tag{6}$$

$$\sigma = \frac{4P}{\pi d_p^2 \delta} \tag{7}$$

where δ is known as a constraint factor. For a given class of materials, δ is a constant [2, 3, 6] and it increases from a value of 1.12 at the initial yielding of the material up to a value near 3 at full plastic zone development. δ is calculated by the ABI software by iterating the following set of equations:

$$\delta = \begin{cases} 1.12 & \phi \le 1 \\ 1.12 + \tau \cdot \ln\phi & 1 < \phi \le 27, \\ 2.87 \cdot \alpha_m & \phi > 27 \end{cases} \tag{8}$$

where

$$\tau = (2.87 \cdot \alpha_m - 1.12)/\ln(27),\ \phi = \varepsilon_p E_{spec}/0.43\sigma_t.$$

There are three stages in the development of the plastic zone beneath the indentation and are expressed analytically in the δ parameter: (i) nucleation of a plastic zone during initial yielding, (ii) development of the zone with an increasing size as a function of ϕ, and (iii) full establishment of plasticity around the indentation as the zone is well developed and envelopes the indentation. The α_m parameter is material dependent and is held constant between 1.10 and 1.25 for various structural steels.

Under compressive loading, materials do not undergo necking and so do not attain instability conditions. Hence the ultimate tensile stress is determined in an indirect way. Since n is equal to the true uniform strain at the ultimate tensile stress of the material under tensile loading, the true ultimate tensile stress can be obtained from Equation 4 as

$$\sigma_{TS} = K(n)^n \tag{9}$$

The ultimate tensile strength (nominal value), S_{UTS}, is then obtained from the equation

$$S_{UTS} = K\left(\frac{\varepsilon_u}{e}\right)^n = K\left(\frac{n}{e}\right)^n, \qquad e \approx 2.71 \tag{10}$$

Values of n and K are determined by regression analysis of the data fitted to Equation 4.

3.3. Indentation energy to fracture (IEF)

Application of ABI technique to determine fracture energy is based on the premise that although compressive loading does not promote fracture, it does introduce a stress concentration in the material through the indentation process. From finite element analysis, it was shown that a tensile stress state existed at the center of the impression just ahead of the indenter [10]. This stress increases in magnitude as the indenter penetrates into the material. Just as conventional destructive fracture tests require a tensile stress concentration at a crack tip, ball indentation introduces an analogous tensile stress concentration albeit over a larger (less sharp) area than a crack tip.

The model assumes fracture conditions to occur if the stress concentration produced by the ball indentation exceeds the material's *critical* cleavage fracture stress (σ_f). (In the case of HSLA steels, it has been established that the critical cleavage fracture stress is independent of temperature and heat-treatment [11]). Hence if the value of stress at the point of maximum stress concentration is known as a function of indentation depth, the depth at which the stress exceeds σ_f could be predicted. If the energy deposited in the material by the indenter could be determined as a function of the depth, then the energy upto assumed fracture stress could be predicted. This energy to fracture is termed the Indentation Energy to Fracture (IEF) [7].

Determination of IEF requires: (i) relationship between ABI flow stress and indentation depth, (ii) relationship between ABI flow stress and stress at the point of stress concentration, (iii) value of the critical stress for cleavage fracture, and (iv) relationship between energy deposited into the material by the indenter and depth of penetration. The relationship between ABI flow stress and depth is obtained from ABI data since load versus depth data is converted into stress versus strain. This relationship, illustrated in Fig. 4, is linear as explained earlier, thereby allowing easy extrapolation.

Using elasticity theory, the ratio between ABI derived flow stress and the maximum stress concentration was estimated to be approximately 2/3 [7]. This ratio was used to relate the critical fracture stress and a representative stress. Instead of converting the flow stress into values of the stress concentration, σ_f was converted into an ABI flow stress called the *representative* fracture stress (σ_f^r) [7],

$$\sigma_f^r = \frac{2}{3}\sigma_f, \tag{11}$$

The representative stress, as defined in Equation 11 is the critical stress to fracture normalized to ABI flow stress and it intersects the flow curve regression line at a corresponding depth value as shown in Fig. 4. This value of depth delineates the point at which the stress state for fracture would exist ahead of the indenter and is termed "depth to fracture (h_f)". IEF, or the energy deposited into the material at the fracture depth is given by integration of ABI flow stress up to the predicted depth to fracture. This energy is in the form of a surface energy, with units of energy per unit area (mJ/mm^2).

The derivation assumes that the flow stress is equal to the mean (or Meyers) stress, i.e., $\sigma_t = P/(\frac{\pi}{4}d^2)$. Load is equal to the slope of the load depth curve, m_{LD}, times the depth, i.e., $P = m_{LD} \cdot h$. Diameter of the impression is calculated from the depth of penetration using Pythagorean's theorem, i.e., $d = \sqrt{Dh - h^2}$. The

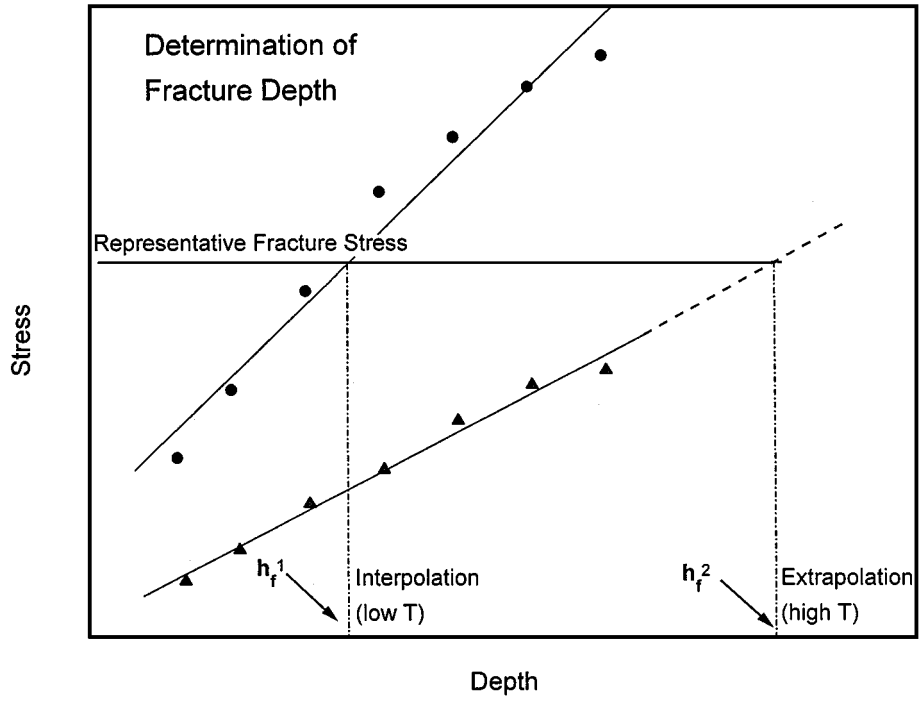

Figure 4 Determining fracture depth from stress vs. depth data.

resultant expression for IEF is in terms of a natural logarithm of the depth to fracture,

$$IEF = \int_0^{h_f} \sigma_t(h)\,dh, \qquad (12a)$$

or,

$$IEF = \int_0^{h_f} \frac{m_{LD} \cdot h}{\pi \cdot (Dh - h^2)}\,dh$$
$$= \frac{m_{LD}}{\pi} \cdot \ln\left[\frac{D}{(D - h_f)}\right], \qquad (12b)$$

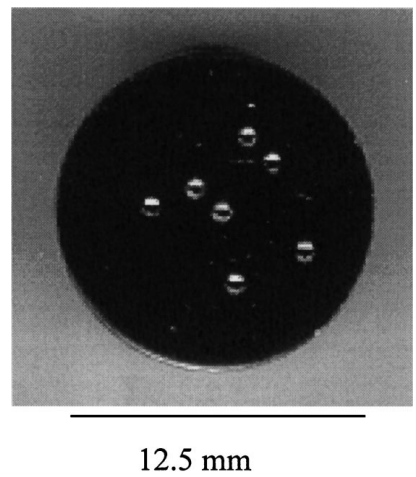

Figure 5 Typical ball indentations from .76 mm diameter ball.

4. Experimental procedure

Automated ball indentation tests were performed using a bench model Stress Strain Microprobe, PortaFlow-P1, developed and patented by M/s Advanced Technology Corporation, USA. A tungsten carbide spherical indenter of 0.76 mm diameter was used for all the tests. ABI tests were carried out at eleven different temperatures in the range from 136 to 423 K on a piece of commercially pure molybdenum metal. An indenter velocity of 0.025 mm/s was selected for all the tests. Cooling of the specimen below room temperature was achieved using liquid nitrogen along with an advanced temperature controller that can control temperature in the range of 73 to 473 K. The indentation load and the corresponding depth were measured on-line using a load cell and LVDT respectively. Tests at all the temperatures could be completed on a single cross-section of the rod since ABI test produces only a small impression. Typical indentations from ABI tests are shown in Fig. 5 while the microstructure of the molybdenum metal is included in Fig. 6.

5. Results and discussion

Fig. 7 shows a comparison of the true-stress versus true-strain curves at various temperatures obtained from the ABI tests. A systematic increase in the flow stress with decrease in temperature is clearly noted. The basic premise in the application of ABI technique is that the material behaves similarly under tensile and compressive loading. The yield stress, ultimate tensile strength, and the work hardening parameters of the material are evaluated from the flow curve. Figs 8 and 9 show the variations of n and K with temperature. n showed a marginal increase with increasing temperature. On the other hand, K decreased continously with increasing temperature over the entire range of values.

The variation of ultimate tensile strength with temperature is shown in Fig. 10. UTS decreased drastically with increase in test temperature; the reduction was by a factor of 3 over the temperature range from 148 to

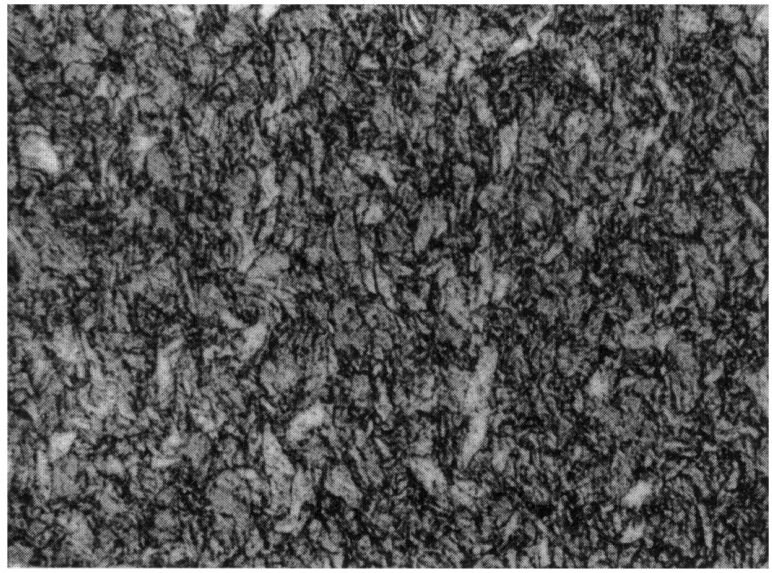

Figure 6 Microstructure of molybdenum in the as-received condition (magnification 100X).

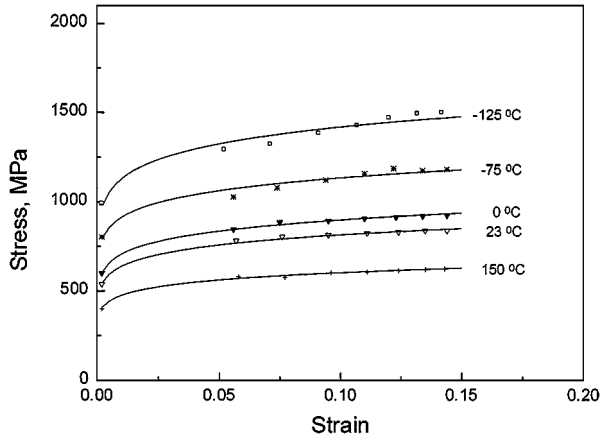

Figure 7 Effect of test temperature on the true-stress true-strain curve.

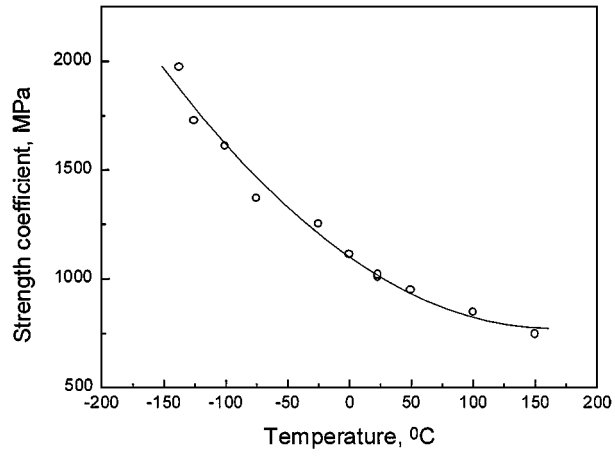

Figure 9 Decrease in strength coefficient with temperature.

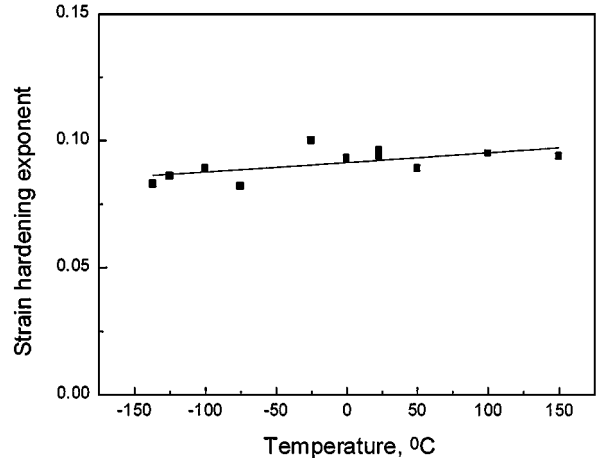

Figure 8 Increase in strain hardening exponent with temperature.

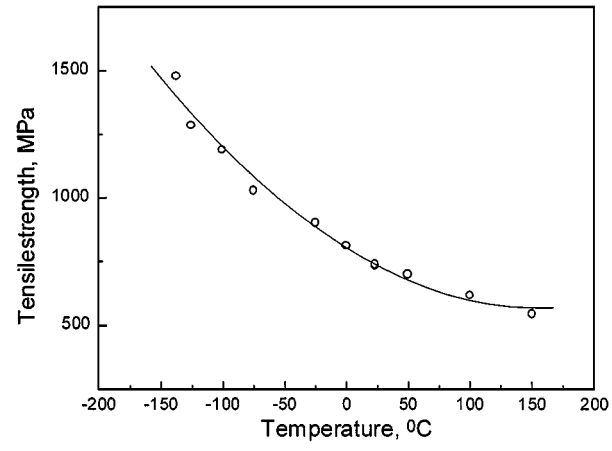

Figure 10 Variation of UTS with temperature.

423 K. The tensile and impact properties of molybdenum are known to depend strongly on the composition, product form and processing conditions [12, 13]. Hence, a comparison of the present results with published data from conventional tensile tests, although scarce, is not easy. Ultimate tensile strength values as low as 500 MPa to as high as 1050 MPa have been reported at room temperature depending upon the purity levels and processing conditions [12]. The present ABI tests yielded a value of 730 MPa which is comparable

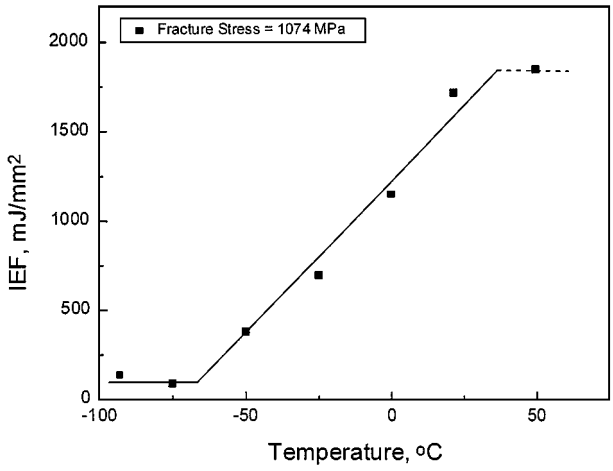

Figure 11 Variation of IEF with temperature.

with the published values, especially about 700 MPa reported for bar products at room temperature in the Metals Handbook [13].

Fig. 11 shows the variation of IEF with temperature over the range of temperatures from 148 to 423 K. In the calculation of IEF, a value of 1075 MPa has been chosen for the true stress to fracture. Fig. 11 clearly demonstrates that the newly developed ABI energy parameter delineates the ductile to brittle transition which is expected in bcc metals such as molybdenum. The transition occurs in the temperature range of 223 to 298 K. It may however be noted that IEF has units of millijoules per sq.mm unlike Charpy energy which has units of Joules. The data at and beyond room temperature are shown with dashed lines to emphasize the fact that in the upper shelf region, the critical fracture stress model is not valid and one needs to incorporate a critical fracture strain criterion [14]. In the absence of reliable published data on the variation of impact energy with temperature, comparison of the transition region with Charpy data has not been carried out.

6. Conclusions

Automated ball indentation technique is an excellent non-destructive tool for characterizing the tensile and fracture properties of materials. The effect of temperature on tensile strength, strain hardening exponent and strength coefficient for bcc molybdenum have been clearly noticed from ABI tests. Ductile to brittle transition has been observed based on the variation of indentation energy to fracture with temperature. These studies suggest that ABI is a very reliable and non-destructive method to monitor shifts in ductile to brittle transition temperature of materials due to changing metallurgical conditions or service exposures.

Acknowledgements

The authors wish to acknowledge Mr. Peter Q Miraglia for experimental help and many valuable discussions. Financial support by research grants from the National Science Foundation (DMR-9504818) and the Department of Energy (through INEEL/university research consortium) is gratefully acknowledged.

References

1. F. M. HAGGAG, U.S. Patent no. 4,852,397 (1989).
2. F. M. HAGGAG and K. L. MURTY, in "Proc. Non-destructive Evaluation and Materials Properties III," edited by P. K. Liaw *et al.* (TMS, 1997) p. 101.
3. F. M. HAGGAG, in "Small Specimen Test Technique Applied to Nuclear Reactor Vessel Thermal Annealing and Plant Life Extension, ASTM STP 1204," edited by W. R. Corwin, F. M. Haggag and W. L. Server (American Society for Testing and Materials, Philadelphia 1993) pp. 27–44.
4. F. M. HAGGAG and R. K. NANSTAD, in "Innovative Approaches to Irradiation Damage and Failure Analysis," edited by D. L. Marriot *et al.* (ASME PVP 1989) Vol.170, p. 41.
5. K. L. MURTY and F. M. HAGGAG, "Investigation of Deformation Characteristics of Electronic Solders using a Novel Stress Strain-Microprobe (SSM): Application to Solder Aging and Life Prediction," Proceedings of InterPACK'97, ASME, EPP-Vol. 19-1, Advances in Electronic Packaging—1997, Vol. 1, pp. 1133–1139.
6. P. Q. MIRAGLIA, MS thesis, North Carolina State University, 1997.
7. F. M. HAGGAG, THAK-SANG BYUN, J. H. HONG, P. Q. MIRAGLIA and K. L. MURTY, *Scripta Met. Mater.* **38** (1998) 645.
8. D. TABOR, "The Hardness of Metals" (Oxford University Press, New York, 1951).
9. V. TIRUPATAIAH and G. SUNDARARAJAN, *Mater. Sci. Eng.* **91** (1987) 169.
10. J. H. UNDERWOOD, G. P. O'HARA and J. J. ZALINKA, *Experimental Mechanics* **27** (1986) 379.
11. P. BOWEN, S. G. DRUCE and J. F. KNOTT, *Acta Metall.* **35** (1987) 1735.
12. L. NORTHCOTT, "Molybdenum" (Butterworths Scientific Publication, 1956) p. 58.
13. Metals Handbook, Vol. 2 (American Society for Metals, 1978) p. 773.
14. R. O. RITCHIE, W. L. SERVER and R. A. WULLARET, *Met. Trans.* **10A** (1979) 1557.

Received 6 February
and accepted 26 October 1998